IEEE Access
Multidisciplinary | Rapid Review | Open Access Journal

Received September 18, 2020, accepted September 25, 2020, date of publication September 30, 2020,
date of current version October 13, 2020.

Digital Object Identifier 10.1109/ACCESS.2020.3027813

High Gain and Low-Profile Stacked Magneto-Electric Dipole Antenna for Phased Array Beamforming

HYUN-JUN DONG, YE-BON KIM, (Member, IEEE), JINGON JOUNG, (Senior Member, IEEE), AND HAN LIM LEE, (Member, IEEE)
School of Electrical and Electronics Engineering, Chung-Ang University, Seoul 06974, South Korea

Corresponding author: Han Lim Lee (hanlimlee@cau.ac.kr)

This research was supported by the National Research Foundation of Korea (NRF) grant funded by the Korea government (MSIT) (2018R1A4A1023826).

ABSTRACT A high gain stacked antenna based on a planar magneto-electric dipole structure is proposed. The main radiator is configured by a probe-fed patch with a symmetrically arranged pair of dipole radiation elements. Further, an additional air-gapped radiator with multiple patch elements is integrated for gain enhancement. Since both the main and stacked radiators are planar structures, the overall volume can remain low-profile regardless of the airgap. To verify the performance of the proposed structure, a single magneto-electric dipole antenna and three different types of stacked radiators were implemented at 5.8 GHz. The magneto-electric dipole antenna showed measured 10-dB impedance bandwidth and gain of 5.2% and 8.0 dBi, respectively with the overall size of $0.96\,\lambda_0 \times 0.96\,\lambda_0$ including a ground plane. With the additional stacked radiator having the airgap of $0.1\,\lambda_0$, the maximum measured gain was increased to 9.6 dBi. Further, to verify the beamforming performances, three types of 1×8 phased array stacked structures were fabricated with a volume of $0.96\,\lambda_0 \times 6.38\,\lambda_0 \times 0.14\,\lambda_0$ at 5.8 GHz. The measurements showed a maximum peak gain of 18.1 dBi and a half-power-beamwidth scan angle of 49° with a side-lobe level less than −8 dB.

INDEX TERMS Antenna gain enhancement, beamforming antenna, low-profile stacked antenna, magneto-electric dipole, phased array antenna.

I. INTRODUCTION

With the increased use of portable devices and wireless sensors, the need for highly efficient battery performance or battery-less devices has been rapidly accelerated. Since the proximity charging based on inductive wireless power transfer (WPT) method has shown a successful adoption in a mobile market, wireless power charging (WPC) for long distance has also gained even more attention than ever. To realize the long-distance wireless charging, microwave power transmission (MPT) has been considered as a promising solution. Among many different building blocks in MPT technology, the challenges in antenna are considered as a bottleneck since the overall system efficiency and physical size depend on antenna. To avoid high loss in microwave-to-DC conversion, electromagnetic (EM) wave propagation path loss should be also minimized. That is, high directivity is required to improve propagation efficiency and thus the beamforming by array antennas is considered as a key technique in MPT. Although the antenna directivity can be improved by increasing the array size, the physical system size, the number of RF parts connected to the array elements and required power consumption will eventually increase as well. Therefore, a high directivity antenna element must be adopted to MPT application to optimize both physical size and efficiency. Further, the beamforming architecture should be adopted to enhance the MPT coverage and operation flexibility. Then, several antenna structures previously reported for gain enhancement might be considered as possible candidates in MPT beamforming applications.

To achieve high gain, cavity or slot-loaded structures have been studied [1]–[3], but insufficient gain with respect to high profile cavity or impractical geometry at high frequency make them unsuitable. Other structures based on periodic

The associate editor coordinating the review of this manuscript and approving it for publication was Sotirios Goudos.

or Yagi-like structures have been also reported [4]–[6], but they require large physical dimension and high profile with respect to ground plane. Further, stacked structures based on planar patch radiators have been proposed [7], [8], but the gain enhancement ratio with respect to the overall volume including the stack height and ground plane size seems to be less effective. Also, many magneto-electric dipole antenna structures with gain and bandwidth enhancement have been studied [9]–[17]. However, these structures require either air-gapped feed line, high profile, metallic sidewalls, large ground plane size, or high volume dielectric resonant materials. Further, since most of these structures are non-planar, the implementation difficulty in a large array makes them impractical. Lastly, a planar type magnetic dipole antenna with high gain has been reported [18]. However, since the structure requires precise via placement, the fabrication and electrical tuning are inevitably difficult. Further, the required antenna dimension is asymmetric, where one side is very long and thus potentially causes an impractical implementation for array configuration. More importantly, the aforementioned antenna structures have not been investigated as array configurations. Especially, there have been few previous reports for magneto-electric dipole antenna array with beam steering characteristics to verify the practical adoption of magneto-electric dipole antennas in future phased array applications. Therefore, in this article, a high gain stacked antenna based on a planar magneto-electric dipole structure with relatively low profile, ease of fabrication and suitability at high frequency is proposed. Further, the proposed antenna is extended to 1×8 array configuration to verify the feasibility of the proposed structure for phased array applications.

II. ANALYSIS AND DESIGN OF THE PROPOSED MAGNETO-ELECTRIC DIPOLE STACKED ANTENNA

Fig. 1 shows the proposed antenna structure consisting of a main antenna on lower substrate and three possible types of patch stacks on upper substrate. The main antenna is configured by a rectangular patch with a signal excitation port and a dual planar electric dipole arranged concentrically. The dual electric dipole consists of four conductors with shorting pins at each corner near the rectangular patch to additionally induce a pair of magnetic dipole excitation. Then, the total operation follows the complementary antenna consisting of the electic dipole and the magnetic dipole placed orthogonally. Thus, the simultaneous excitation of the dipole pairs provides the electro-magnetic dipole radiation with a gain enhancement. Further to increase the antenna directivity, the air-gapped stack with symmetrically distributed patch elements is adopted as shown in Fig. 1. Here, the lower and upper elements are separated by four plastic spacers. To view the fundamental design approaches, an equivalent circuit model as shown in Fig. 2 can be referred. The main patch antenna has a fundamental resonant mode represented by a parallel-RLC circuit whereas the additional conductors as an electric dipole can be represented by a series-RLC circuit.

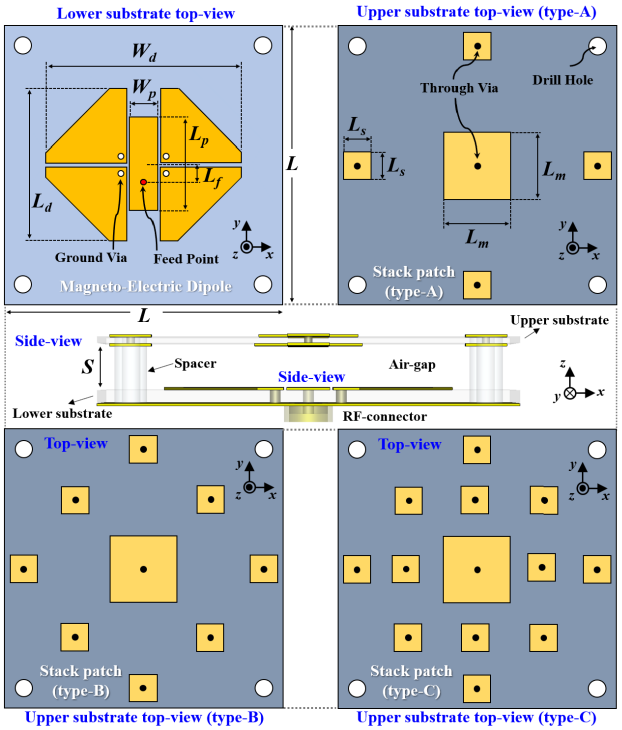

FIGURE 1. The proposed structures with the magneto-electric dipole (single antenna), stack type-A, type-B and type-C antennas.

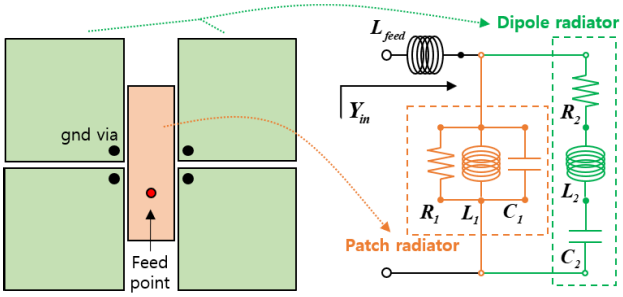

FIGURE 2. Equivalent circuit model of a simple magneto-electric dipole antenna with simplified RLC elements.

Having a shorting-via through each additional conductor, magnetic resonance can be further adjusted in addition to the main patch antenna. According to Fig. 2, L_{feed} represents the reactance by feed line and thus can be omitted for the magneto-electric operation principles. For the ease of analysis, if R_1, L_1 and C_1 are assumed to include the magnetic dipole loading effect, the approximate input admittance excluding L_{feed} can be expressed as follows.

$$Y_{in} \simeq \left(\frac{1}{R_1}+\frac{1}{R_2}\right) - j\omega\left[\frac{1}{R_2^2}\left(L_2-\frac{1}{C_2}\right)-\left(C_1-\frac{1}{L_1}\right)\right] \quad (1)$$

Here, if $C_2L_2 = C_1L_1$ is satisfied, the imaginary part of the equation (1) can be cancelled. That is, if the patch radiator and electric dipole have the same resonant frequency, the complementary operation of magneto-electric dipole antenna

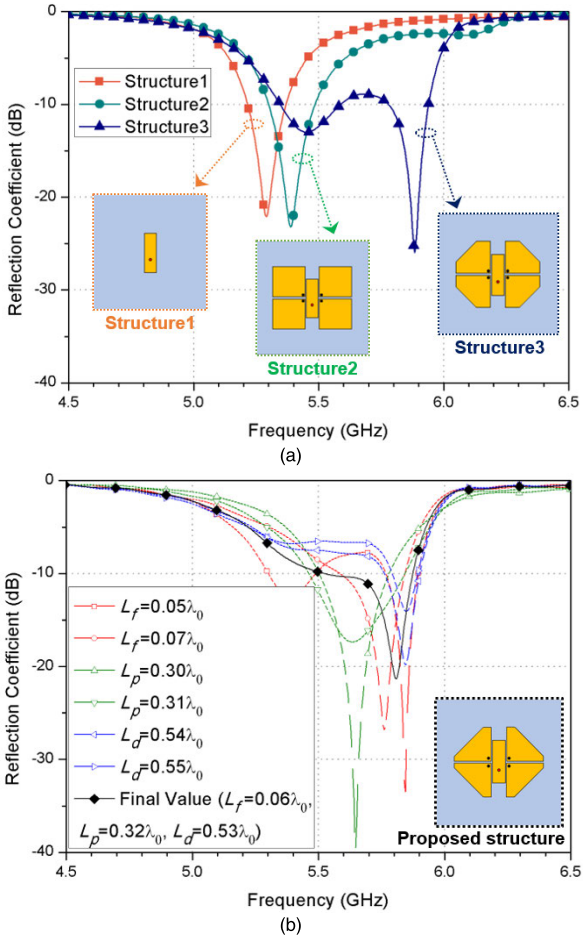

FIGURE 3. Simulated results for (a) structural behaviors and (b) fine tuning of the proposed magneto-electric dipole antenna.

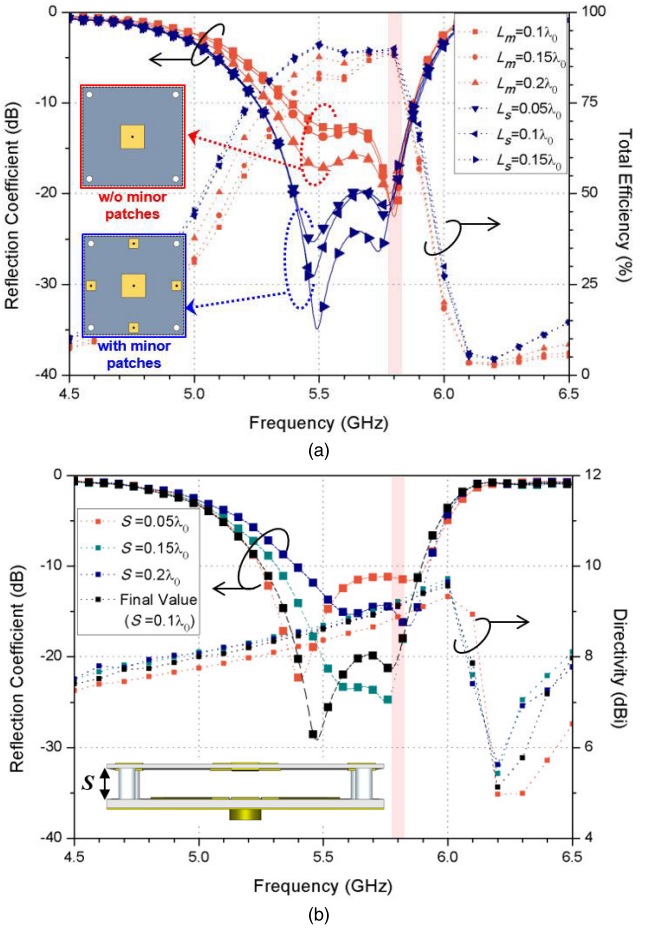

FIGURE 4. Simulated results for (a) reflection coefficient and efficiency based on the stack pattern, and (b) reflection coefficient and directivity based on the spacing between the lower and upper substrates.

at a desired frequency can be achieved. Thus, the proposed antenna design can be started with designing a simple patch antenna operating near the target frequency. Then, additional concentric conductors with shorting-vias as dipole radiators can be placed near the patch to adjust the resonance frequency. This design process can be quickly conducted by the simulation as shown in Fig. 3 (a), where Taconic substrate with a dielectric constant of 2.5 and a loss tangent of 0.0019 is used. A single rectangular patch is designed at a frequency slightly lower than a target frequency of 5.8 GHz. Having the ground plane size set to 0.96 λ_0 x 0.96 λ_0, additional four shorted conductors are closely placed around the rectangular patch to shift the operation frequency slightly higher. Here, the initial physical size of the shorted conductors is chosen to be intentionally large to increase the achievable gain. Then, cutting the edges of the four shorted conductors shifts the center frequency further and increases the bandwidth as well. The variation in reflection coefficient according to the changes in geometric parameters defined in Fig. 1 are shown in Fig. 3 (b). Once the single magneto-electric dipole antenna is optimized, the effect of planar air-gapped stack patch is further investigated as shown in Fig. 4.

Firstly, a single patch stack is added above the magneto-electric dipole antenna with an arbitrary space of 0.1λ_0. Then, L_m value for the main stack patch is optimized to have both enhanced gain and bandwidth. Further, the additional minor patches with the dimension defined by L_s are concentrically placed around the main stack patch and optimized as well, as shown in Fig. 4 (a). To implement electrically thick conductors, the identical stack patches are printed on both the top and bottom sides of the upper substrate and connected through vias. When the stack with the minor patches are used, the bandwidth is extended to about 11.1% while the bandwidth for the stack without the minor patches are 8.5 %. Also, the simulated total efficiency with the L_m of 0.2 λ_0 and *Ls* of 0.1 λ_0 is found to be 90% at 5.8 GHz. Secondly, the spacing between the lower magneto-electric dipole and the upper stack patches is optimized as shown in Fig. 4 (b). Although the maximum directivity of 9.2 dBi is observed at S of 0.15 λ_0, the bandwidth is slightly smaller than the case having S of 0.1 λ_0 where the directivity is 9.1 dBi. Thus, the spacing of 0.1 λ_0 is selected instead of 0.15 λ_0 regarding both the physical volume and electrical characteristics including the bandwidth. Based on the simulated results,

TABLE 1. Geometric parameters of the proposed antenna.

Parameters	Value (mm)	Parameters	Value (mm)
L	50.0	L_f	3.0
L_d	27.2	L_m	12.0
W_d	34.8	L_s	5.0
W_p	5.2	S	5.0
L_p	16.7	-	-

the optimized parameters' physical values are summarized in Table 1.

Having the optimized parameters, different stack types are also simulated. Referring to Fig. 1, the type-A, type-B and type-C stacks correspond to the number of minor patches with four, eight and twelve, respectively. With the increased number of minor patches around the major stack patch, the directivity also increases while the total efficiency decreases slightly. Since type-B and type-C have more minor patches compared with the type-A, the capacitive loading effect results the quality factor to slightly decreased and thus the total efficiency gets also slightly decreased. The simulated results for different antennas with the same ground plane size are summarized in Table 2.

TABLE 2. Comparison of the simulated results at 5.8 GHz.

Antenna type	Impedance bandwidth (%)	Peak directivity (dBi)	Total efficiency (%)
Conventional Patch	4.0	7.6	81.6
Magneto-electric	6.2	8.3	87.1
Stack type-A	10.9	9.1	90.1
Stack type-B	10.9	9.2	89.5
Stack type-C	10.7	9.4	85.2

Comparing the single magneto-electric dipole antenna with the conventional patch, the impedance bandwidth, directivity and efficiency are all improved. By adopting the air-gapped stack type-A, all of the electrical characteristics are further enhanced. Also, stack type-B and type-C shows slight increase in directivity in turn of slight decrease in efficiency. Further to confirm the electromagnetic performances of the proposed antennas, 3-D EM simulations are also conducted by CST Microwave Studio for the single magneto-electric dipole and three types of the air-gapped stacked antennas. According to Fig. 5 (a), the main patch drives the electric dipole with highly concentrated surface currents along the patch at t of 0. Further, the magnetic dipole across the shorted conductors are driven as shown at t of T/4. Fig. 5 (b) shows the coupled electric field from the lower antenna to the upper stack, resulting in the enhanced field directivity. Fig. 5 (c) shows the induced surface currents for different stack types as well.

To further investigate the beamforming performance of the proposed structures, the 1 × 8 magneto- electric dipole

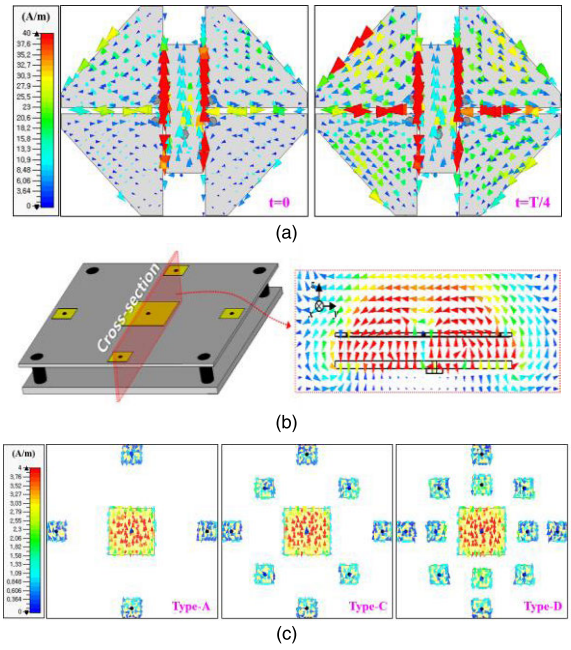

FIGURE 5. 3D-EM simulated results for (a) surface currents of the magneto-electric operation, (b) electric field cross-sectional view and (c) induced surface currents on different upper stack types.

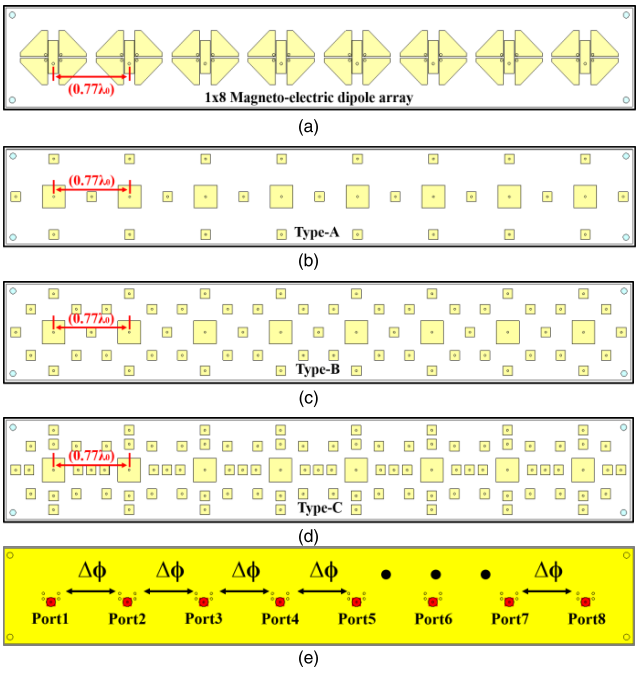

FIGURE 6. The 1 × 8 array with the (a) magneto-electric dipole elements, (b) type-A, (c) type-B, (d) type-C stacked configurations and (e) bottom view with a relative phase shift ($\Delta\phi$).

arrays with type-A, type-B and type-C stacked configurations are simulated by the same software, CST as shown in Fig. 6. The simulated array dimension including the ground plane is 0.96 λ_0 × 6.38 λ_0 with the element center-to-center spacing of 0.77 λ_0 and the airgap of 0.1 λ_0. The simulated results show the maximum peak gains of 18.2 dBi, 18.3 dBi

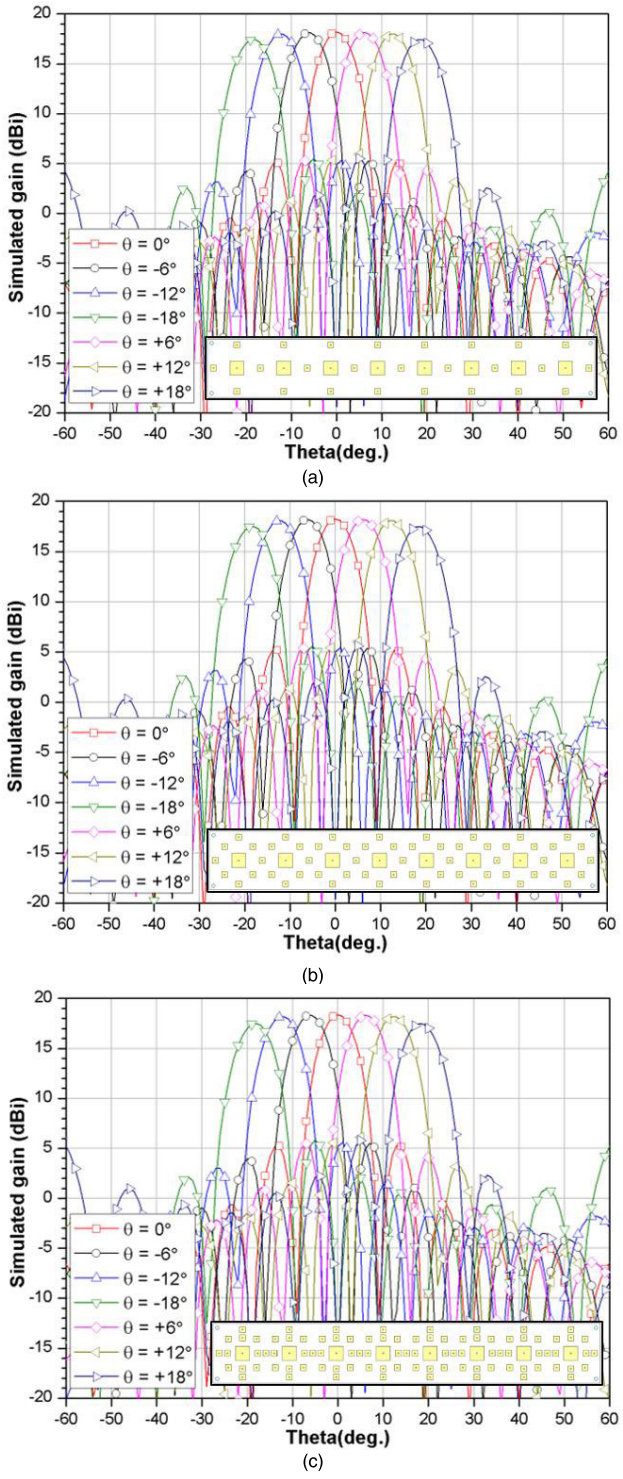

FIGURE 7. The simulated 1 × 8 array beam patterns for the (a) type-A, (b) type-B and (c) type-C stacked configuration at 5.8 GHz.

and 18.4 dBi for type-A, type-B and type-C, respectively as shown in Fig. 7. The main beam steering angle while maintaining the side-lobe level (SLL) less than −10 dB is about 36° for all types.

Within the main beam steering range, the peak gain variation is less than 0.9 dB for all types. Further, having a

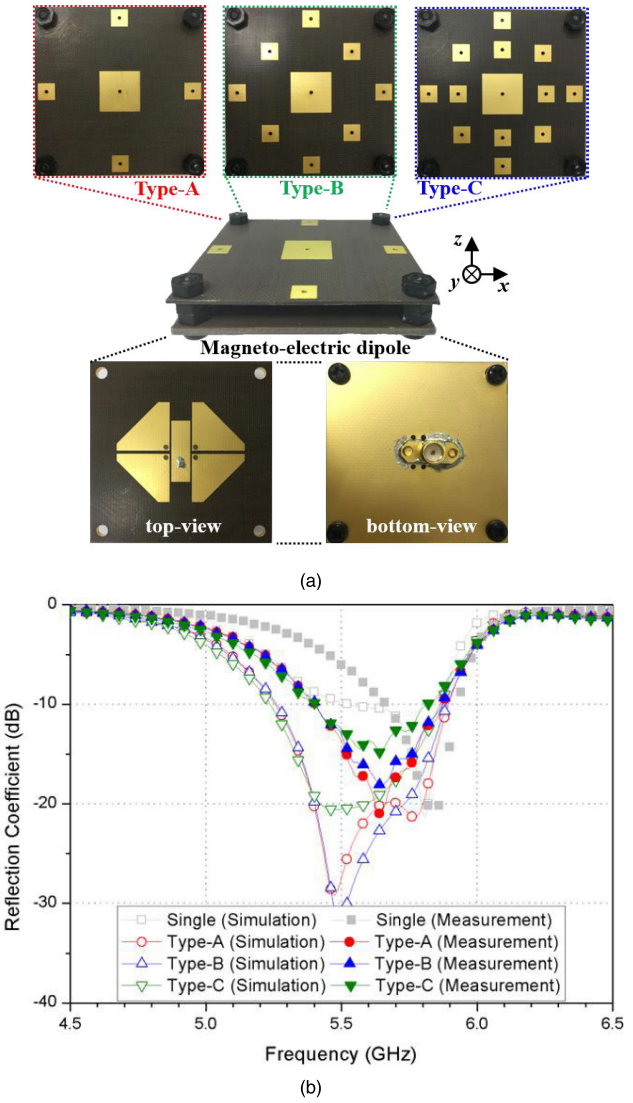

FIGURE 8. (a) Implementation of the proposed single antennas with different views, and (b) simulated and measured reflection coefficients of the proposed single magneto-electric dipole and stacked antennas.

half power beamwidth (HPBW) as a criterion to determine the maximum beam steering angle, all types show 46° scan angles while keeping the SLL less than −10 dB.

III. FABRICATION AND MEASUREMENT FOR THE PROPOSED ANTENNA ARRAY

The proposed antennas were fabricated with a Taconic TLX-9 substrate having a dielectric constant of 2.5 and a loss tangent of 0.0019 as shown in Fig. 8 (a). The substrate thicknesses for the lower antenna and the upper stack were 1.57 mm and 0.79 mm, respectively. Having the ground plane of 50 × 50 mm^2 and the air-gapped spacing of 5 mm, the overall volume of the proposed stacked antenna at 5.8 GHz was about 0.96 λ_0 × 0.96 λ_0 × 0.14 λ_0. Fig. 8 (b) shows the simulated and measured reflection coefficients of the single magneto-electric dipole, stack type-A, type-B and type-C antennas. The measured 10-dB impedance bandwidth of the type-A,

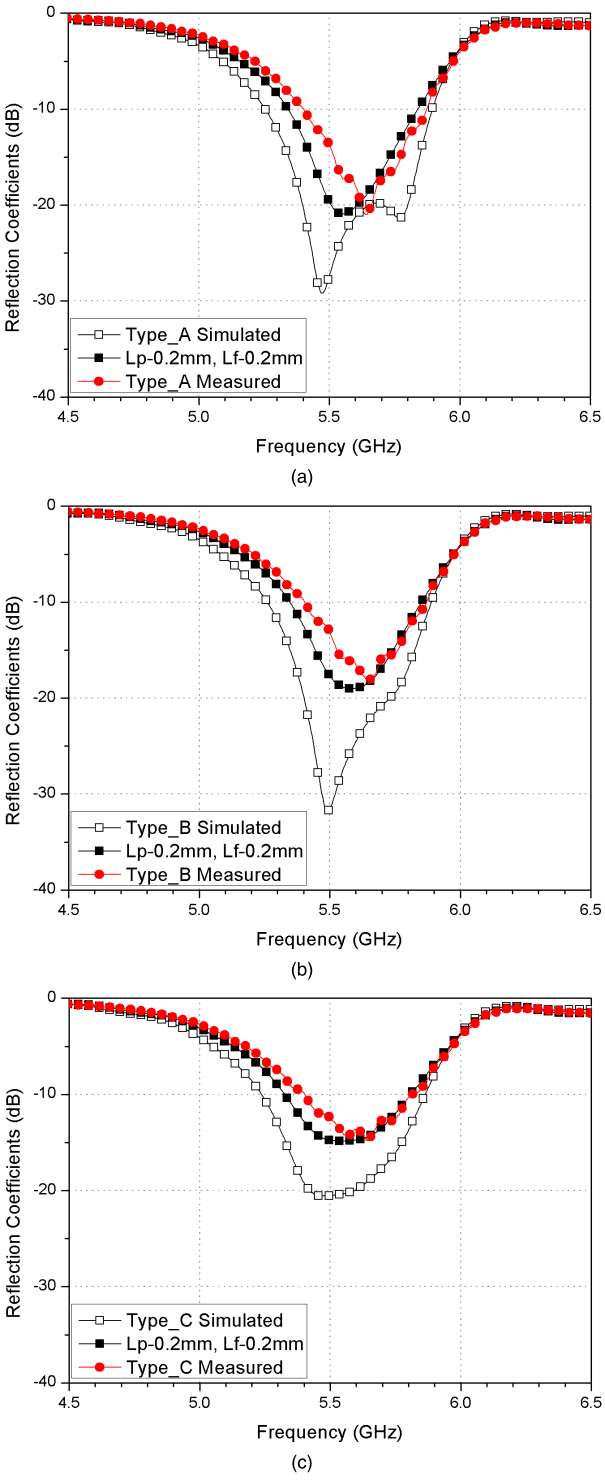

FIGURE 9. Simulated reflection coefficients of the (a) type-A, (b) type-B and (c) type-C for error analysis with Lp and Lf parameter offsets.

type-B, and type-C were 8.1%, 7.9%, and 7.2%, respectively. The measurement showed a reduction in bandwidth compared with the simulated results due to the fabrication error. Thus, the simulation analysis was also conducted to verify the deviation in design parameters. By trial and error, both

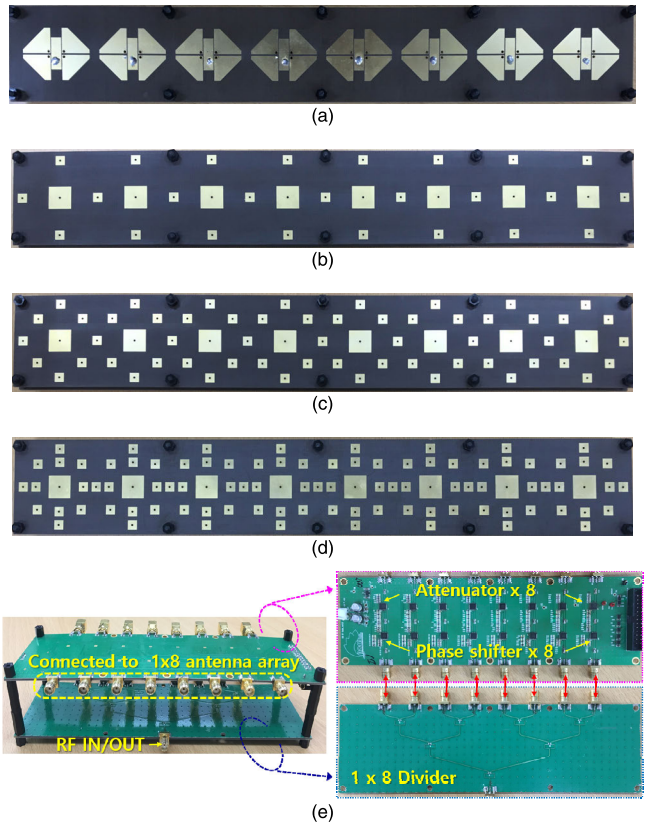

FIGURE 10. Implementation of the 1 × 8 (a) magneto-electric dipole, (b) type-A, (c) type-B, (d) type-C stacked arrays and (e) beamforming module configured by 1 × 8 Wilkinson divider, attenuators and phase shifters.

L_p and L_f were found to be approximately 0.2 mm-smaller than the desired values as shown in Fig. 9. The simulated results with 0.2 mm offsets for both L_p and L_f values showed a reasonable agreement with the measured results for all types. Although the measured bandwidths were slightly narrower than the simulated bandwidths, all types showed improved bandwidths with respect to the conventional patch. Further, 1 × 8 array antennas with the beamforming module configured by a 1 × 8 Wilkinson divider, eight attenuators and eight phase shifters to drive each radiation element were implemented as shown in Fig. 10. Each stacked array antenna dimension was 0.96 λ_0 × 6.38 λ_0 × 0.14 λ_0 at 5.8 GHz. Regarding the beamforming module, the measured insertion loss of the divider was about 1 dB and the loss variation among each port was less than 0.1 dB at 5.8 GHz. The reflection coefficients for all ports were always better than 15 dB from 5.4 to 6.2 GHz. Further, commercially available 6-bit RF digital phase shifters (MAPS-011008) and digital attenuators (MAAD-000523) were used to control the magnitude and phase for each antenna element. To validate the operation band and coupling among each antenna element within the 1 × 8 stacked array, the simulated and measured reflection coefficients and isolation for selected antenna elements were compared as shown in Fig. 11. The measured minimum 10-dB impedance bandwidths for type-A, type-B

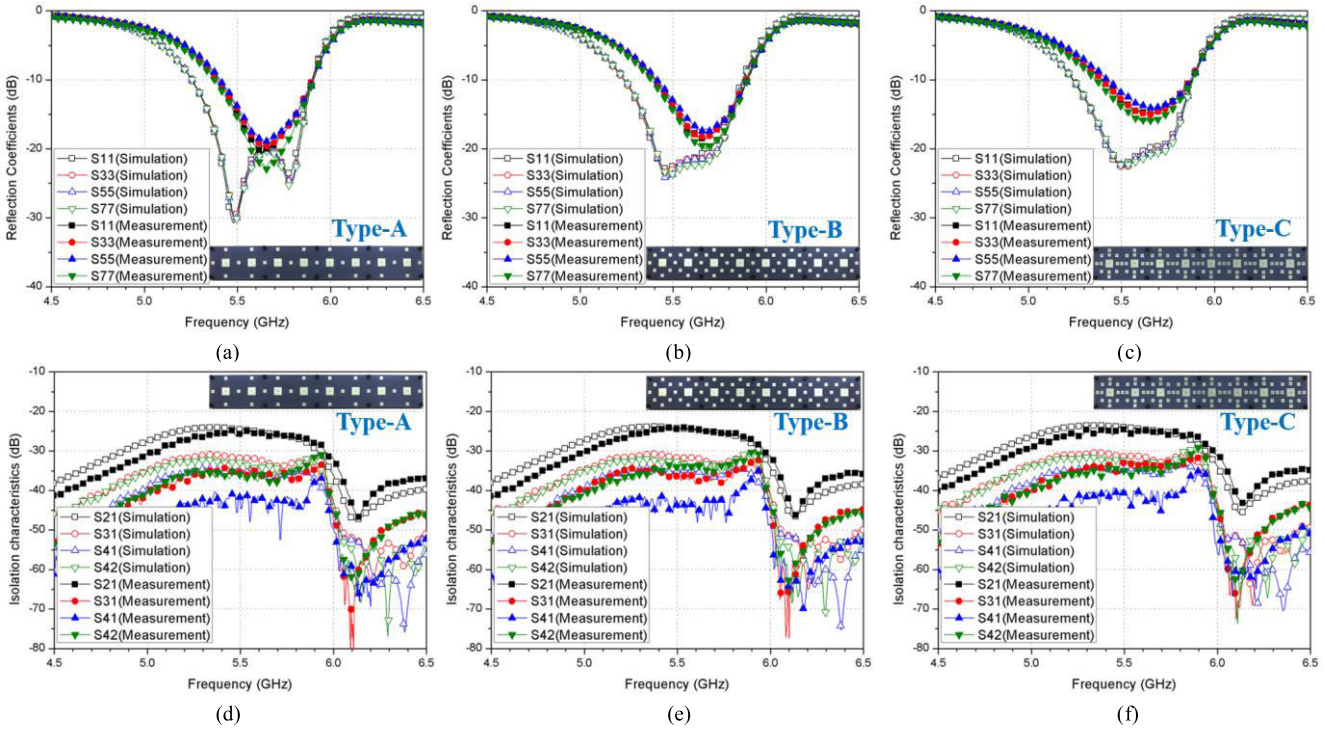

FIGURE 11. The simulated and measured S-parameters for (a)-(c) reflection coefficients and (d)-(f) isolation characteristics of the 1 × 8 type-A, type-B and type-C stacked arrays.

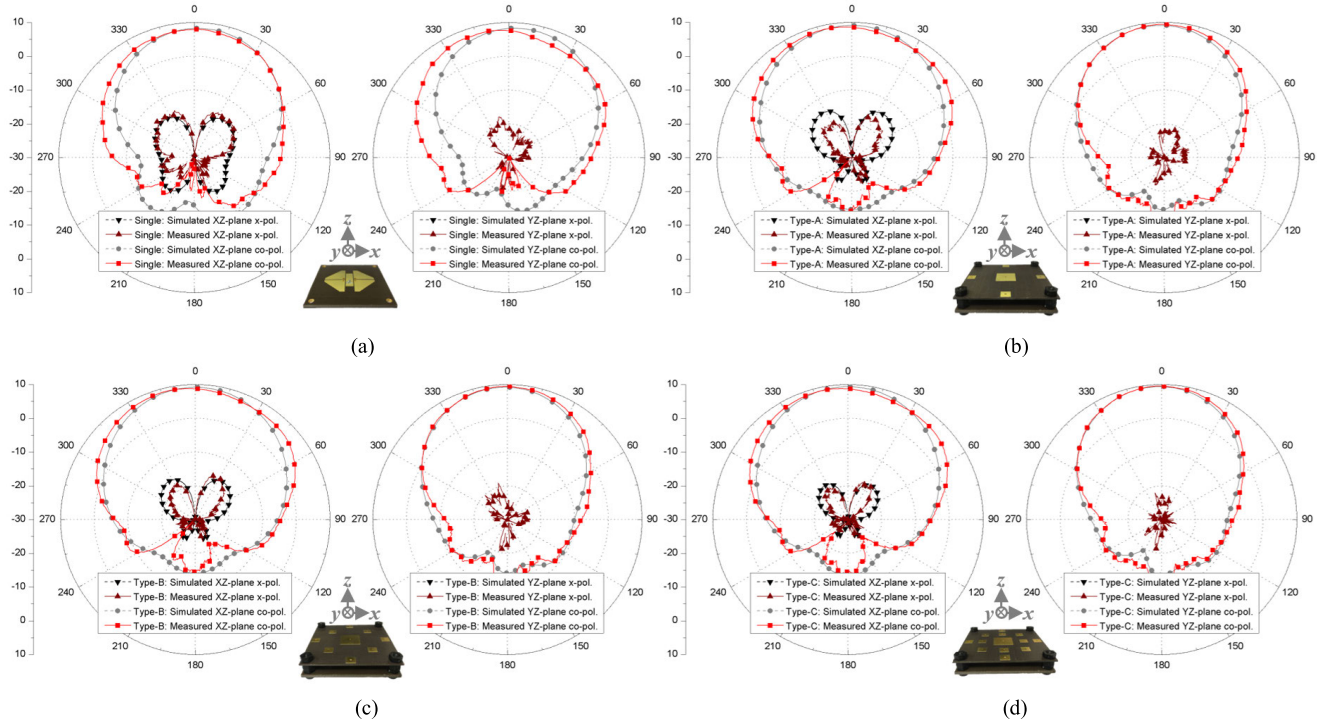

FIGURE 12. Measured radiation patterns of the proposed antennas in xz-plane and yz-plane at 5.8 GHz: (a) single magneto-electric dipole, (b) stack type-A, (c) stack type-B and (d) stack type-C antennas.

and type-C stacked array antennas were 8.8%, 8.1%, and 7.9%, respectively. The measured minimum isolations among each antenna element within the 10-dB impedance bandwidth for type-A, type-B and type-C stacked array were about 26.6 dB, 25.9 dB and 25.8 dB, respectively. Thus, the measured S-parameters for all types showed a good agreement

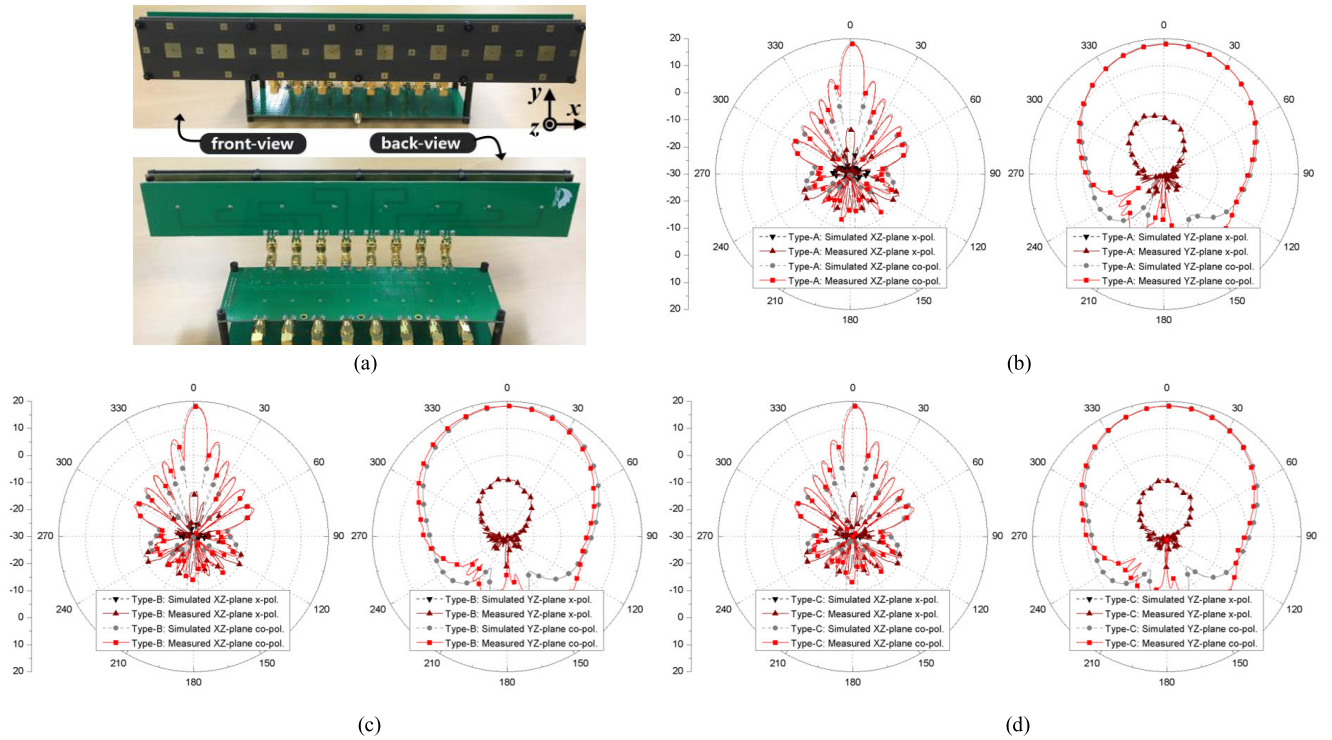

FIGURE 13. Measured radiation patterns of the proposed array in xz-plane and yz-plane at 5.8 GHz: (a) fabricated beamforming antenna module, (b) type-A, (c) type-B and (d) type-C stacked array.

TABLE 3. Performance comparison of the proposed antenna.

Ref.	Antenna geometry	Total volume including ground plane (λ_0^3)	Realized peak gain [dBi(c)]	Center frequency (GHz)	Impedance bandwidth (%)	Realized gain / volume [dBi(c)/λ_0^3]
[9]	Non-planar	$1.64\lambda_0$ x $1.64\lambda_0$ x $0.23\lambda_0$	8.0	4.1	85	12.9
[10]	Non-planar	$1.15\lambda_0$ x $1.15\lambda_0$ x $0.21\lambda_0$	7.0	3.5	11.4	25.2
[11]	Non-planar	$1.09\lambda_0$ x $1.09\lambda_0$ x $0.45\lambda_0$	8.2	3.2	65	15.3
[12]	Non-planar	$1.00\lambda_0$ x $1.00\lambda_0$ x $0.15\lambda_0$	11.0	1.6	48	73.3
[13]	Non-planar	$0.80\lambda_0$ x $0.80\lambda_0$ x $0.18\lambda_0$	8.2	2.4	33.3	71.1
[14]	Non-planar	$1.01\lambda_0$ x $1.01\lambda_0$ x $0.16\lambda_0$	9.7	2.3	41	58.2
[15]	Non-planar	$1.85\lambda_0$ x $1.85\lambda_0$ x $0.26\lambda_0$	9.4	3.9	37	10.6
[16]	Non-planar	$1.10\lambda_0$ x $1.10\lambda_0$ x $0.22\lambda_0$	7.8	2.2	55.4	29.3
[17]	planar	$0.75\lambda_0$ x $0.75\lambda_0$ x $0.11\lambda_0$	8.2	3.8	27.6	132.5
[18]*	planar	$0.66\lambda_0$ x $2.13\lambda_0$ x $0.03\lambda_0$	10.2	10.3	9.1	241.8
This work: without** / with stack type-C	planar	$0.96\lambda_0$ x $0.96\lambda_0$ x $0.03\lambda_0$ / $0.96\lambda_0$ x $0.96\lambda_0$ x $0.14\lambda_0$	8.0 / 9.6	5.8	5.2 / 7.2	289.4 / 74.4

*magnetic dipole; **non-stacked magneto-electric dipole

with the simulated results. Then, the radiation patterns in both xz and yz planes of the proposed single antennas were firstly measured at 5.8 GHz as shown in Fig. 12. The measured peak gains were 8.0 dBi and 7.9 dBi, respectively in xz and yz planes for the unstacked single magneto-electric dipole antenna as shown in Fig. 12 (a). The measured HPBWs were 77.0° and 78.0° in xz and yz planes, respectively. Fig. 12 (b) shows the measured peak gains of 8.8 dBi and 9.5 dBi, respectively in xz and yz planes for the stacked type-A antenna. The measured HPBWs were 99.0° and 64.0° in xz and yz planes, respectively. Fig. 12 (c) shows the measured peak gains of 9.0 dBi and 9.5 dBi, respectively in xz and yz planes for the stacked type-B antenna. The measured HPBWs were 96.0° and 64.0° in xz and yz planes, respectively. Also, Fig. 12 (d) shows the measured peak gains of 9.0 dBi and 9.6 dBi, respectively in xz and yz planes for the stacked type-C antenna. The measured HPBWs were 96.0° and 62.0° in xz and yz planes, respectively.

Further, the proposed 1 × 8 beamforming antenna module was integrated as shown in Fig. 13 (a). The radiation patterns

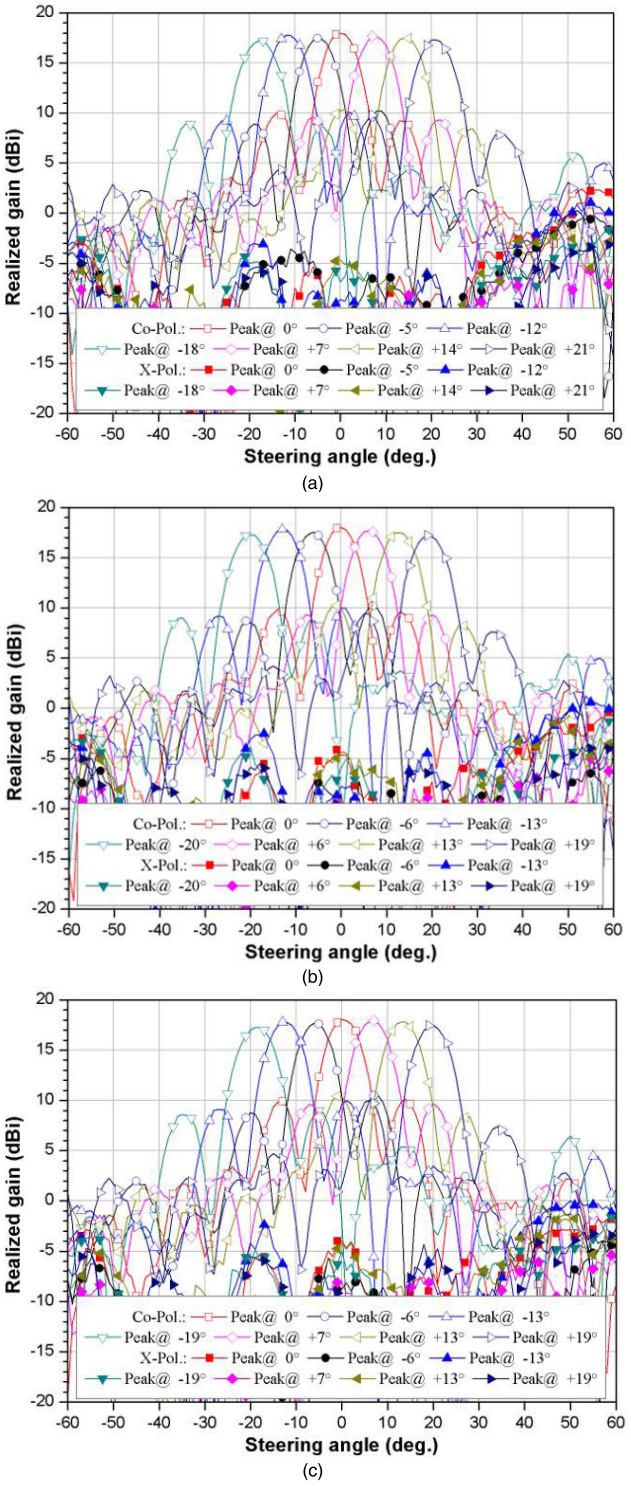

FIGURE 14. Measured beamforming performances of the fabricated 1 × 8 (a) type-A, (b) type-B and (c) type-C stacked arrays in xz-plane.

for main beams at the center were first measured in both xz and yz planes at 5.8 GHz. Then, after the beamforming circuit loss was compensated, the measured results were compared with the simulated results as shown in Fig. 13 (b)-(d). The measured array peak gains with the circuit loss compensation for type-A, type-B and type-C configurations were 17.9 dBi, 18.0 dBi, and 18.1 dBi, respectively. The HPBW in xz planes for all types was 8°. Also, The HPBWs in yz planes for type-A, type-B and type-C configurations were 63°, 62° and 61°, respectively. To compare the proposed antenna performance with the other state-of-the-art magneto-electric dipole antennas, the realized gain-to-volume ratio is summarized with the other electrical characteristics in Table 3. Here, the proposed single planar non-stacked magneto-electric dipole antenna showed the highest realized gain-to-volume ratio including the magnetic dipole antenna. Although the type-C stacked antenna showed a reduction in the gain-to-volume ratio, it showed an excellent ratio among the magneto-electric dipole antennas. Finally, the beam steering performances of the proposed structures were measured as shown in Fig. 14. The measured beam steering angles with respect to the main beam positions for type-A, type-B and type-C stacked arrays were 39°, 39° and 38°, respectively with the SLL kept less than −8.0 dB. Here, the peak gain variations during the beam steering for all types were less than 0.8 dB. Further, the measured HPBW scan angles maintaining SLL less than −8.0 dB for type-A, type-B and type-C stacked arrays were 49°, 49° and 48°, respectively. Therefore, the measured beamforming performances showed a good agreement with the simulated results and demonstrated the proposed architectures as a good candidate for beamforming applications.

IV. CONCLUSION

In this paper, a high gain stacked antenna based on a planar magneto-electric dipole structure was proposed and verified at 5.8 GHz. The total volume of the proposed single stacked antenna including the air-gap was 0.96 λ_0 × 0.96 λ_0 × 0.14 λ_0. The proposed single antenna showed the enhanced bandwidth, peak gain and efficiency with the maximum peak gain was about 9.6 dBi with a 7.2% operation bandwidth. Further, three types of 1 × 8 stacked array structures with the identical volume of 0.96 λ_0 × 6.38 λ_0 × 0.14 λ_0 were fabricated and integrated with the phased array beamformer. The measured beamforming performances of the proposed antenna module showed the maximum peak gain of 18.1 dBi with a 7.9% operation bandwidth. Also, the maximum beam steering angles regarding the main beam position and HPBW with the SLL kept less than −8.0 dB were 39° and 49°, respectively.

REFERENCES

[1] Q. Yang, X. Zhang, N. Wang, X. Bai, J. Li, and X. Zhao, "Cavity-backed circularly polarized self-phased four-loop antenna for gain enhancement," *IEEE Trans. Antennas Propag.*, vol. 59, no. 2, pp. 685–688, Feb. 2011.

[2] R. Bayderkhani, K. Forooraghi, and B. Abbasi-Arand, "Gain-enhanced SIW cavity-backed slot antenna with arbitrary levels of inclined polarization," *IEEE Antennas Wireless Propag. Lett.*, vol. 14, pp. 931–934, Dec. 2015.

[3] J. Wei, X. Jiang, and L. Peng, "Ultrawideband and high-gain circularly polarized antenna with double-Y-shape slot," *IEEE Antennas Wireless Propag. Lett.*, vol. 16, pp. 1508–1511, Jan. 2017.

[4] W. Cao, B. Zhang, A. Liu, T. Yu, D. Guo, and Y. Wei, "Broadband high-gain periodic endfire antenna by using I-Shaped resonator (ISR) structures," *IEEE Antennas Wireless Propag. Lett.*, vol. 11, pp. 1470–1473, Dec. 2012.
[5] Y. Liu, H. Liu, M. Wei, and S. Gong, "A novel slot Yagi-like multilayered antenna with high gain and large bandwidth," *IEEE Antennas Wireless Propag. Lett.*, vol. 13, pp. 790–793, Apr. 2014.
[6] H. Wang, S.-F. Liu, L. Chen, W.-T. Li, and X.-W. Shi, "Gain enhancement for broadband vertical planar printed antenna with H-shaped resonator structures," *IEEE Trans. Antennas Propag.*, vol. 62, no. 8, pp. 4411–4415, Aug. 2014.
[7] V. P. Sarin, M. S. Nishamol, D. Tony, C. K. Aanandan, P. Mohanan, and K. Vasudevan, "A wideband stacked offset microstrip antenna with improved gain and low cross polarization," *IEEE Trans. Antennas Propag.*, vol. 59, no. 4, pp. 1376–1379, Apr. 2011.
[8] X. Y. Zhang, W. Duan, and Y.-M. Pan, "High-gain filtering patch antenna without extra circuit," *IEEE Trans. Antennas Propag.*, vol. 63, no. 12, pp. 5883–5888, Dec. 2015.
[9] X. Cui, F. Yang, M. Gao, L. Zhou, Z. Liang, and F. Yan, "A wideband magnetoelectric dipole antenna with microstrip line aperture-coupled excitation," *IEEE Trans. Antennas Propag.*, vol. 65, no. 12, pp. 7350–7354, Dec. 2017.
[10] Z.-Y. Zhang and K.-L. Wu, "A wideband dual-polarized dielectric magnetoelectric dipole antenna," *IEEE Trans. Antennas Propag.*, vol. 66, no. 10, pp. 5590–5595, Oct. 2018.
[11] J. Tao, Q. Feng, G. A. E. Vandenbosch, and V. Volskiy, "Director-loaded magneto-electric dipole antenna with wideband flat gain," *IEEE Trans. Antennas Propag.*, vol. 67, no. 11, pp. 6761–6769, Nov. 2019.
[12] C. Ding and K.-M. Luk, "A low-profile dual-polarized magneto-electric dipole antenna," *IEEE Access*, vol. 7, pp. 181924–181932, Dec. 2019.
[13] S. Gao, H. Lin, L. Ge, and D. Zhang, "A magneto-electric dipole antenna with switchable circular polarization," *IEEE Access*, vol. 7, pp. 40013–40018, Mar. 2019.
[14] L. Cai, H. Wong, and K.-F. Tong, "A simple low-profile coaxially-fed magneto-electric dipole antenna without slot-cavity," *IEEE Open J. Antennas Propag.*, vol. 1, pp. 233–238, May 2020.
[15] J.-N. Sun, J.-L. Li, and L. Xia, "A dual-polarized magneto-electric dipole antenna for application to N77/N78 band," *IEEE Access*, vol. 7, pp. 161708–161715, Nov. 2019.
[16] G. Zhang, L. Ge, J. Wang, and J. Yang, "Design of a 3-D integrated wideband filtering magneto-electric dipole antenna," *IEEE Access*, vol. 7, pp. 4735–4740, Nov. 2019.
[17] S. J. Yang, Y. M. Pan, Y. Zhang, Y. Gao, and X. Y. Zhang, "Low-profile dual-polarized filtering magneto-electric dipole antenna for 5G applications," *IEEE Trans. Antennas Propag.*, vol. 67, no. 10, pp. 6235–6243, Oct. 2019.
[18] Y. Shi and J. Liu, "Investigation of a via-loaded microstrip magnetic dipole antenna with enhanced bandwidth and gain," *IEEE Trans. Antennas Propag.*, vol. 67, no. 7, pp. 4836–4841, Jul. 2019.